

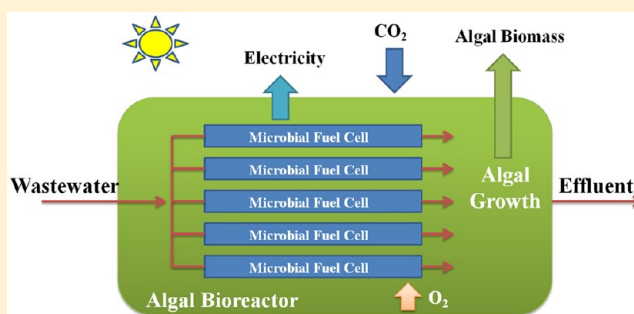
Integrated Photo-Bioelectrochemical System for Contaminants Removal and Bioenergy Production

Li Xiao,[†] Erica B. Young,^{‡,§} John A. Berges,^{‡,§} and Zhen He^{†,*}

[†]Department of Civil Engineering and Mechanics, [‡]Department of Biological Sciences, and [§]School of Freshwater Sciences, University of Wisconsin-Milwaukee, Milwaukee, Wisconsin 53211, United States

Supporting Information

ABSTRACT: An integrated photobioelectrochemical (IPB) system was developed by installing a microbial fuel cell (MFC) inside an algal bioreactor. This system achieves the simultaneous removal from a synthetic solution of organics (in the MFC) and nutrients (in the algal bioreactor), and the production of bioenergy in electricity and algal biomass through bioelectrochemical and microbiological processes. During the one-year operation, the IPB system removed more than 92% of chemical oxygen demand, 98% of ammonium nitrogen, and 82% of phosphate and produced a maximum power density of 2.2 W/m³ and 128 mg/L of algal biomass. The algal growth provided dissolved oxygen to the cathode reaction of the MFC, whereas electrochemical oxygen reduction on the MFC cathode buffered the pH of the algal growth medium (which was also the catholyte). The system performance was affected by illumination and dissolved oxygen. Initial energy analysis showed that the IPB system could theoretically produce enough energy to cover its consumption; however, further improvement of electricity production is desired. An analysis of the attached and suspended microbes in the cathode revealed diverse bacterial taxa typical of aquatic and soil bacterial communities with functional roles in contaminant degradation and nutrient cycling.



INTRODUCTION

Municipal wastewater treatment plants play a critical role in environmental protection, but the operation of such plants consumes an extensive amount of energy.¹ An ongoing challenge to sustainability is to improve the efficiency of wastewater management to reduce energy demands and to increase energy recovery from waste. To address this challenge, the key research tasks include optimizing a more energy-efficient process of removing dissolved organics from wastewater and reducing aeration, which represents an important, electricity-demanding step in most municipal wastewater treatment facilities; developing better processes for capturing the energy bonded within the organic contaminants of wastewater to produce electric energy; and improving nutrient (chiefly inorganic nitrogen and phosphorus) removal/recovery from wastewater by using a process that consumes fewer resources (e.g., aeration required for nitrification,² and chemicals for denitrification and phosphorus precipitation). These key challenges have been addressed in various ways, but primarily in distinct and separated approaches (e.g., anaerobic digesters and algal bioreactors in different locations). A system that aims to integrate these approaches may increase efficiency, and save energy and resources.

To achieve such a system, we can synergistically link microbial fuel cells (MFCs)³ with algal bioreactors⁴ for wastewater treatment and bioenergy production. MFCs will

remove organics and provide nutrients and carbon dioxide to grow algae in the bioreactor, and algal bioreactors will remove nutrients and provide dissolved oxygen to the MFC cathode reaction. MFCs can effectively remove various organic substrates,⁵ but nutrient removal is generally limited under an anaerobic condition with a few specially designed nutrient removal processes.^{2,6–9} Algal treatment of wastewater has a long history, especially in removing nutrients, and provides additional services by using photosynthesis to fix carbon dioxide into organic compounds for fuel biomass production.¹⁰ Microalgae can assimilate significant amounts of nutrients because of high N and P demand for synthesis of proteins (45–60% of microalgae dry weight), nucleic acids, phospholipids, and other cellular constituents.¹¹ The algal biomass produced from bioreactors also can be used for producing biofuels, including biodiesel.^{12,13}

Linking MFCs to algal growth can be accomplished in several ways. First, algal biomass can be used as a fuel in MFCs, but the efficiency of energy production is very low due to the low transfer of chemical energy from algae to electrochemically active bacteria.^{14,15} Second, electrodes can be installed in algal

Received: August 2, 2012

Revised: September 21, 2012

Accepted: September 21, 2012

Published: September 21, 2012

bioreactors for electricity generation;¹⁶ however, mixing algae with electrochemically active bacteria will adversely affect anode reactions because of dissolved oxygen produced by algae,¹⁷ and the presence of organic compounds will stimulate the growth of heterotrophic bacteria that compete with algae for nutrients. Third, MFCs and algal bioreactors can be installed separately and the algal bioreactor can receive MFC effluent; in this way, the intrinsic problems with each process are not solved. For instance, in a membrane-based MFC, its cathode requires an additional supply of water and oxygen, as well as pH buffering, and algal bioreactors need pH buffering when CO₂ is added.

To address these intrinsic problems, we have developed an integrated photobioelectrochemical (IPB) system. Instead of simply connecting the two processes in series, the IPB system involves a unique integration of MFCs within an algal bioreactor, leading to a potentially more efficient system that can achieve both waste treatment and bioenergy production (Figure 1). In this system, wastewater is fed into the MFCs

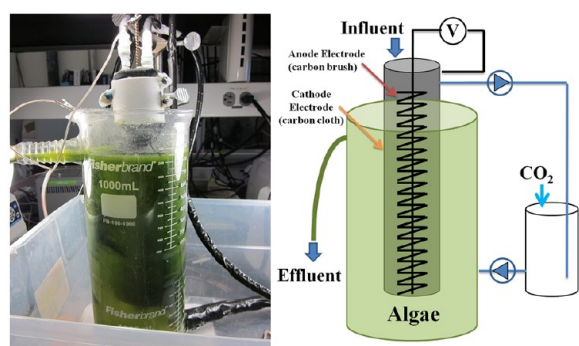


Figure 1. Experimental setup (left) and schematic (right) of the IPB system.

where organic contaminants are oxidized; the remaining inorganic nutrients are then discharged into the algal bioreactor for algal growth, which strips nutrients out of the water before the treated effluent is released for final tertiary treatment (e.g., disinfection). Installing MFCs inside an algal bioreactor would have algae producing oxygen used by the MFCs for their cathode reactions, thereby reducing the need for aeration. If additional CO₂ (e.g., waste gas from power plants) is added to the algal bioreactor for algal growth, the pH of the algal growth medium could become acidic, thereby inhibiting algal growth; MFC cathodic reactions can buffer the pH by adding alkalinity resulting from oxygen reduction. Through this combination, the two treatment processes are cooperatively linked for the same purpose of treating wastewater, with two different bioenergy products: bioelectricity from the MFCs, and algal biomass for use in biofuels production.

In this study, we operated a bench-scale IPB system for more than 360 days with three primary objectives: (1) to examine the long-term system performance of organic/nutrient removal and energy production; (2) to understand the effects of illumination or aeration on the IPB system; and (3) to understand the microbial composition of the biofilm attached on the cathode electrode and planktonic cells in the cathode compartment (algal bioreactor).

MATERIALS AND METHODS

IPB System Setup. The IPB system consisted of a single-chamber tubular MFC installed in a glass beaker, which

functioned as both the cathode compartment and the algal bioreactor (Figure 1). The MFC was constructed based on a cation exchange membrane tube (CEM, Ultrex CMI7000, Membranes International, Inc., Glen Rock, NJ) with a diameter of 4.5 cm and a height of 20 cm, resulting in an anode liquid volume of ~300 mL. A 20 cm long carbon brush (Gordon Brush Mfg. Co., Inc., Commerce, CA) was used as the anode electrode. Before use, the carbon brush electrode was pretreated by immersing in acetone overnight and heating at 450 °C for 30 min. The cathode electrode was a layer of carbon cloth with Pt/C as catalysts that wrapped the CEM tube. To coat the Pt catalyst to the cathode electrode, Pt/C powder was mixed with Nafion solution and then applied to the carbon cloth surface with a brush to a final loading rate of ~0.5 mg Pt/cm². The anode and cathode electrodes were connected by copper wires to an external circuit across a 100 Ω resistance. The glass beaker that held the MFC had a diameter of 10 cm and height of 29 cm, with a liquid volume of 1700 mL. Three compact fluorescent bulbs (32 W, 120 V, Energy Wiser, color temperature 4000 K, Bulbrute Industries, Inc., China) were installed around the cathode to provide an average irradiance of 13 W/m² on a 16 h on/8 h off cycle, unless noted elsewhere.

Operating Conditions. The IPB system was continuously operated with a synthetic solution at about 20 °C. The anode compartment was inoculated with the anaerobic sludge from a local municipal wastewater treatment plant (South Shore, Milwaukee, WI). The cathode compartment was initially inoculated with the green algae *Pseudokirchneriella subcapitata* (Korshikov) Hindak (CPCC 37) obtained from the Canadian Phycological Culture Collection (www.phycol.ca) and previously maintained in axenic culture. The synthetic solution had 2.48 mS/cm conductivity and pH of 7.8, and contained (per L of tap water): sodium acetate, 0.35 g; NH₄Cl, 0.2 g; NaCl, 0.5 g; MgSO₄, 0.015 g; CaCl₂, 0.02 g; NaHCO₃, 0.6 g; KH₂PO₄, 0.027 g and 1 mL/L of trace elements.¹⁸ This solution was fed into the anode of the MFC at a flow rate of 0.4 mL/min (with an anolyte recirculation rate of 30 mL/min), resulting in a hydraulic retention time (HRT) of 12.5 h and an organic loading rate of 0.51 kg COD/m³/d in the anode compartment. The effluent of the anode flowed into a 500 mL beaker where CO₂ was bubbled by a gas diffuser to provide inorganic carbon for algal growth and then pumped into the cathode of the MFC at the same flow rate of the anode feeding. The catholyte was mixed by a magnetic stirrer.

Measurement and Analysis. The cell voltage was recorded every 5 min by a digital multimeter (2700, Keithley Instruments, Inc., Cleveland, OH). Power density and current density was based on the anode liquid volume, according to a previous study.¹⁸ The calculations of Coulombic efficiency (CE), Coulombic recovery (CR), and energy consumption are shown in the Supporting Information (SI). The concentrations of soluble COD, ammonium nitrogen, nitrite nitrogen, nitrate nitrogen, and phosphate were measured according to the manufacturer's instructions using a DR/890 datalogging colorimeter (Hach Company, Loveland, CO). The pH, temperature, and dissolved oxygen (DO) were measured using a 556 MPS hand-held multiparameter instrument (YSI Incorporated, Yellow Spring, OH). The concentration of algal mass was measured as absorbance at 680 nm in a 1100 spectrophotometer (Unico, Dayton, NJ) and converted to biomass using the standard curve shown in SI Figure S1. The procedures of scanning electron microscopy and cathode microbial analysis are shown in the SI.

RESULTS AND DISCUSSION

Performance of the IPB System. The IPB system was operated for more than 360 days and its electricity production was affected by illumination and organic input (SI Figure S2). In the first 30 days, the COD concentration of the anode influent was 624 mg/L, which resulted in higher power output (SI Figure S2) than that of the later period that had an influent COD concentration of 266 mg/L. To exhibit more details, electricity production, DO, pH and temperature for a period of 4 days are shown in Figure 2. The electricity produced by the

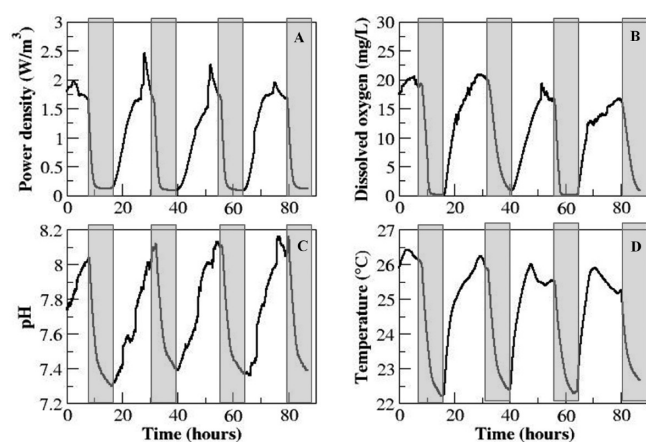


Figure 2. The performance and operating parameters of the IPB system: power density, dissolved oxygen, pH, and temperature. The white indicates the illuminated period and the shadow indicates the dark period.

MFC exhibited a day-night profile, affected by illumination (16 h light: 8 h dark) (Figure 2A). The peak power density reached $2.2 \pm 0.2 \text{ W/m}^3$ under illumination. Because no aeration was provided in this period, the cathode reaction relied on the dissolved oxygen (DO) produced by algae in the cathode compartment. Similar to current generation, the DO concentration varied on a day-night basis, and under illumination DO concentration reached 20 mg/L (Figure 2B), more than twice the saturated DO in DI water at the same temperature, which has been observed in other algal bioreactors.¹⁹ When the light was turned off, the DO gradually dropped to below 1 mg/L, resulting in a power density of $0.1 \pm 0.0 \text{ W/m}^3$ in the dark. Although oxygen in the air could be dissolved in the catholyte and contributed to electricity generation, this contribution was much smaller compared with the algae-produced oxygen, as demonstrated by the low electricity generation in the dark, even with active aeration (Figure 4). Therefore, it is reasonable to conclude that algae can provide a substantial amount of oxygen to the cathode reaction under illumination.

The pH of the catholyte (algal growth medium) varied between 7.3 and 8.2 (Figure 2C), a result of the combined

effect of the cathode oxygen reduction and CO_2 buffering: the MFC cathode reaction could elevate the pH of the catholyte to above 11²⁰ and the anode effluent saturated with CO_2 had a low pH of ~ 4 ; when the low pH anode effluent entered the cathode compartment, the oxygen reduction increased the pH to levels appropriate for algal growth (7–9²¹). On the other hand, the low pH of the anode effluent also benefited the cathode reaction by providing more protons. The addition of CO_2 not only provides carbon source for algal growth, but also buffers the catholyte and thus eliminates the use of an expensive buffer solution that is not practical for large scale application.^{22,23} A potential source of CO_2 is combustion of digester biogas, or flue gas if the MFC system can be installed adjacent to power plants. In addition, biological processes such as nitrification could also provide protons and thus lower the pH of the catholyte. The illumination also changed the temperature of the catholyte with an increase from ~ 22 to ~ 26 °C from dark to under illumination (Figure 2D). Such an increase in temperature could benefit the anode microbes when heat is transferred into the anode compartment through the CEM and electrolyte.

The IPB system effectively reduced the concentrations of both organics and nutrients. The anode removed 92.4% of SCOD and decreased its concentration from 266.7 to $22.0 \pm 13.7 \text{ mg/L}$, which was further reduced to $20.2 \pm 2.9 \text{ mg/L}$ by the cathode (Table 1). The average CE was 7.7%, and the average CR was 7.2%. Almost all of ammonium (98.6%) was removed through either algal uptake or nitrification. It is interesting to note that the anode effluent contained less than half of the initial ammonium concentration; because anaerobic ammonium oxidation has not been well demonstrated in the anode of an MFC,²⁴ we believe that the ammonium loss was due to ammonium transport into the cathode compartment through the cation exchange membrane.⁹ Nitrification was expected to occur in the cathode because of the presence of both dissolved oxygen and bacteria. Denitrification, on the other hand, would be very limited because of the DO. The growth of some algae is faster with ammonium than with nitrate, and the presence of ammonium higher than $1 \mu\text{M}$ could inhibit nitrate uptake,^{25,26} resulting in the observed nitrate accumulation to $19.3 \pm 1.8 \text{ mg/L}$. The removal of total nitrogen by the IPB system was about 63%. The concentration of phosphate was decreased by 82.3% in the IPB system, including a 27% reduction in the anode compartment likely due to the bacterial uptake, and a 55% reduction in the cathode compartment because of the algal uptake. The final phosphate concentration was $1.1 \pm 0.2 \text{ mg/L}$; future studies will include a more detailed analysis of total phosphorus fractions, including organic phosphorus that can be released under an anaerobic condition. The IPB system produced an algal biomass of $128 \pm 36 \text{ mg/L}$ (or 43.37 mg/L/day based on the liquid volume of the algal bioreactor), which was comparable with other algal bioreactors fed on wastewater.¹⁰

Table 1. Characteristics of the Synthetic Solution When Flowing Through the IPB System; the Error Term Is Standard Deviation^a

| | SCOD (mg/L) | $\text{NH}_4^+\text{-N}$ (mg/L) | $\text{NO}_3^-\text{-N}$ (mg/L) | $\text{NO}_2^-\text{-N}$ (mg/L) | $\text{PO}_4^{3-}\text{-P}$ (mg/L) | biomass (mg/L) |
|------------------|-----------------|---------------------------------|---------------------------------|---------------------------------|------------------------------------|----------------|
| anode influent | 266.7 | 52.3 | N/D | N/D | 6.2 | N/A |
| anode effluent | 22.0 ± 13.7 | 20.3 ± 0.5 | N/D | N/D | 4.5 ± 0.2 | N/A |
| cathode effluent | 20.2 ± 2.9 | 0.7 ± 0.8 | 19.3 ± 1.8 | N/D | 1.1 ± 0.2 | 128 ± 36 |

^aN/D: not detected; N/A: not available.

Effects of Illumination on the IPB System. To understand the influence of illumination on the IPB system, we created two scenarios: keeping constant illumination, or increasing the frequency of light/dark cycles. When the illumination was extended to 24 h/day, the power density gradually decreased with time (Figure 3A); within 2 days, the

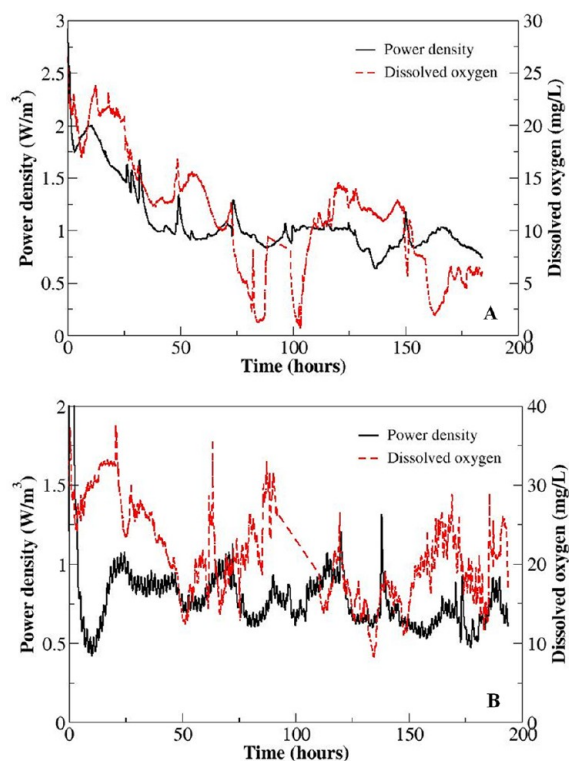


Figure 3. Power density (black solid line) and the DO (red dashed line) during the continuous illumination (A) and the increased light/dark cycle (B).

accumulated electricity production improved, compared with the on/off illumination, but for a period of 7 days, the total electricity production was not much higher (Table 2), because of the low power output after 2 days. Likewise, the DO

Table 2. Energy Production and Consumption in the IPB System under Different Illumination and Aeration Operating Conditions

| | | 16 h on/8 h off (kWh/m ³) | 24 h/d on (kWh/m ³) | 1 h on/0.5 h off (kWh/m ³) | night aeration ^a (kWh/m ³) |
|--------|--------------------------|--|---------------------------------------|---|---|
| input | pump ^b | -0.011 | -0.011 | -0.011 | -0.011 |
| | mixing ^c | -0.057 | -0.057 | -0.057 | -0.057 |
| | aeration | N/A | N/A | N/A | -0.004 |
| output | electricity | 0.012 | 0.013 | 0.010 | 0.021 |
| | biomass ^d | 0.081 | 0.057 | 0.073 | 0.085 |
| net | total | 0.016 | -0.007 | 0.006 | 0.025 |
| | electricity ^e | -0.056 | -0.055 | -0.058 | -0.051 |

^aAeration rate of 30 cc/min and 16 h on/8 h off illumination.

^bEstimated according to hydraulic head loss and theoretic equation (SI). ^cEstimated according to energy consumption by a recirculation rate of 120 mL/min. ^dEnergy consumption during treating algal biomass is not included. ^eExcluding the energy production from biomass.

concentration also decreased. The similar trend between electricity and DO confirmed that photosynthetic O₂ production determined the power density in the IPB system. Research found that some algae require a dark period for division, which could be inhibited by high light intensity and continuous illumination.²⁷ The continuous illumination also promoted nitrification in the catholyte. The highest concentration of nitrate in the effluent during this period was 32.2 mg NO₃⁻-N/L, which was about 1.7 times that of the 19.3 mg NO₃⁻-N/L shown in Table 1. It was previously reported that the presence of algae inhibited the growth of nitrifying bacteria because of faster algal growth rate and toxicity to nitrifiers;²⁸ our results confirmed that decreased photosynthesis (and algal growth) could benefit nitrifying bacteria, as shown by a higher nitrate concentration under constant illumination.

When the frequency of the light/dark cycles was increased to 1 h light/0.5 h dark, the electricity production maintained between 0.5 and 1 W/m³ (Figure 3B). The average DO concentration stayed around 20 mg/L (Figure 3B), much higher than under continuous illumination (Figure 3A), suggesting that the dark condition was beneficial to net algal oxygen production.²⁹ The concentration of nitrate decreased to 17.6 mg/L at the end of the increased light/dark cycle period, suggesting that the improved algal activities slowed down nitrification, compared with continuous illumination.

Aeration in the Dark. We investigated the effects of intermittent aeration (in the dark) on the production of electricity and algal biomass, using three aeration rates, 30, 50, and 100 mL/min (Figure 4). As expected, the aeration

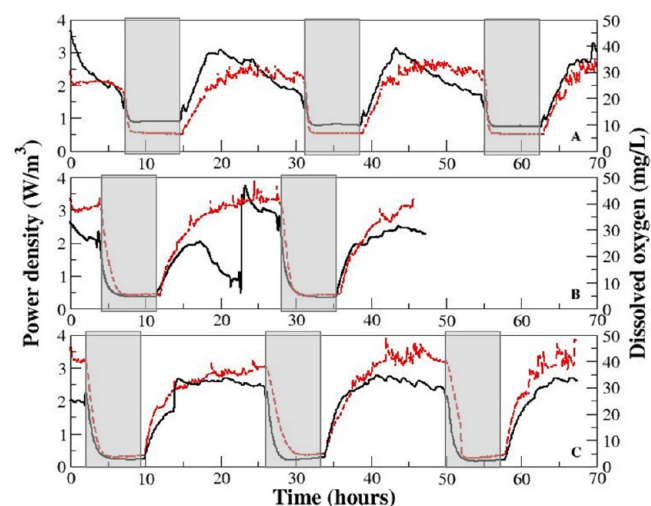


Figure 4. Power density (black solid line) and the DO (red dashed line) during the aeration in the dark at three aeration rates: (A) 100 mL/min, (B) 50 mL/min and (C) 30 mL/min. The shadow indicates the dark period.

increased the DO at night, as well as the power production. At 30 mL/min aeration, the electric power was improved by about 40% compared with no aeration (Table 2). The highest DO in the dark with 100 mL/min aeration was about 8 mg/L (Figure 4A), much lower than during algal photosynthesis under illumination, indicating that algal production of DO would be more promising than mechanical aeration. Aeration also encouraged algal growth and improved biomass production by ~5% (Table 2). However, aeration consumed additional

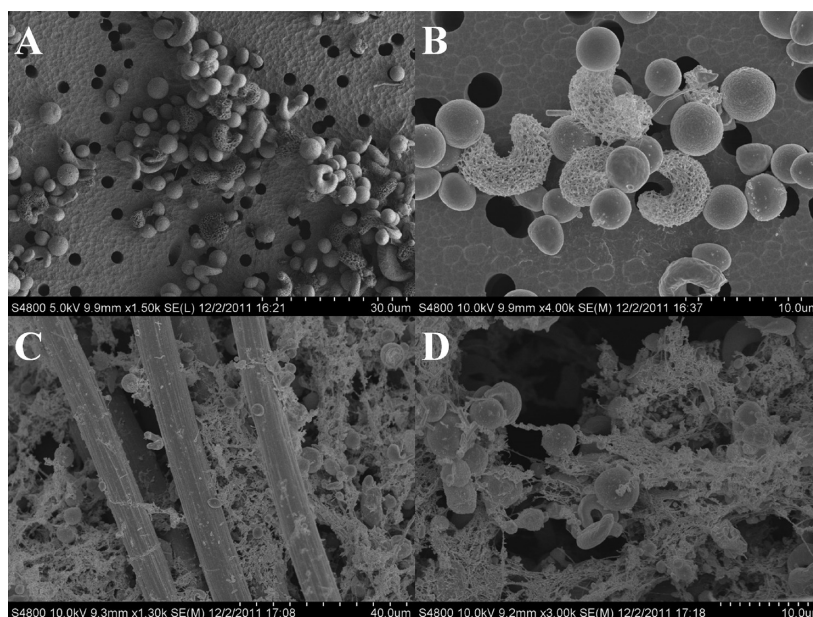


Figure 5. SEM pictures of suspended cells (A and B) collected on filter membrane and biofilm on the cathode electrode (C and D). Note presence of both bacteria and algal cells (spherical *Chlamydomonas reinhardtii* and crescent-shaped *Pseudokirchneriella subcapitata*).

electric energy, so an analysis of energy balance with this approach in the IPB system would be needed.

Energy Balance. Table 2 summarizes energy production and consumption in the IPB system under four different conditions. It must be noted that this is a preliminary analysis and a precise energy analysis is very difficult for a bench-scale system. Energy production consists of two parts, electric energy and biomass energy. Electric energy was calculated according to the power production of the MFC while energy trapped in algal biomass was estimated based on the assumption that biomass contains 20% oil that is converted to biodiesel ($E_{\text{biodiesel}}$ is $\sim 37\,800$ MJ/ton)^{12,30} and a conversion efficiency of 30% from diesel to electricity. Energy consumption was mainly due to the pumping system (recirculation and feeding) and was estimated according to a previous publication³¹ (more details in the SI). The energy consumption of mixing was estimated according to a catholyte recirculation rate of 120 mL/min, which was experimentally found to maintain a similar system performance to that with the mechanic mixing. Energy consumption of the intermittent aeration was estimated according to an aeration efficiency of 1.2 kg O₂/kWh.³²

In general, the IPB system could theoretically produce more energy than it consumed, and the intermittent aeration was beneficial with a larger net energy balance through improving both the electricity generation and the algal growth. The electricity produced in the MFC accounted for 14–29% of the energy consumption, depending on the operating condition. The algal biomass provided much more energy than the MFC. Considering that energy consumption during the conversion of algal biomass to biodiesel was not included in Table 2, the actual energy from algal biomass would be less. If the energy production in the MFC can be improved by 5–10 times to 0.06–0.12 kWh/m³, which may be possible through optimizing configuration and operation, the IPB system will achieve energy neutrality based on the electricity generation alone, with additional economic benefits obtained from the algal biomass. To evaluate the energy benefits of the IPB system, we also need to consider the energy saving. It has been reported that

anaerobic treatment of low-strength wastewater consumes much less energy (e.g., 0.058 kWh/m³ in an anaerobic membrane bioreactor³³) than activated sludge treatment (~ 0.6 kWh/m³³⁴). Therefore, the energy saved by omitting the aeration provides additional significance for the application of an IPB system.

Analysis of Cathode Microbial Communities. Because the anode microbial communities have been well documented,³⁵ in this study we focused on the cathode microbes, which are important to comprehend the interaction and the competition between algae and bacteria. A large number of sequences (up to 50% from each sample) were identified as “chloroplast”, derived from organellar DNA extracted from the chlorophyte algae present in the MFC cathode (*Chlamydomonas reinhardtii* and *Pseudokirchneriella subcapitata*), evident in the SEM images (Figure 5). The source of *C. reinhardtii* could be the anode inocula, or the air because the algal bioreactor was an open system. These chloroplast sequences were not included in the analysis of bacteria.

Of the bacteria present in the biofilm on the cathode electrode, and in the catholyte suspension, there were diverse bacterial taxa representing groups typical of aquatic and soil bacterial communities, shown as pooled taxa from each of three replicates in Figure 6. The dominant classes were the alpha-, beta- and gamma-Proteobacteria along with Acidobacteria_Gp3, which together represented between 68 and 90% of bacterial sequences identified in replicate samples. The family Xanthomonadaceae was the dominant family in all samples, with 49 and 26% of total taxa in pooled samples from membrane and suspension communities, respectively, and a mean of triplicate samples from electrodes of $46.0 \pm 20.2\%$ and $30.7 \pm 5.5\%$ in suspension (SI Figure S3). This was especially due to sequences identified as *Aquimonas*, which was the most abundant genus in both the electrode ($37.5 \pm 23.9\%$) and the suspension communities ($28.1 \pm 6.6\%$) (SI Figure S4). Additional BLAST searches using individual sequences did not clarify which species of this genus were present. *Aquimonas* is a common aquatic bacterial genus, with a capacity for nitrate

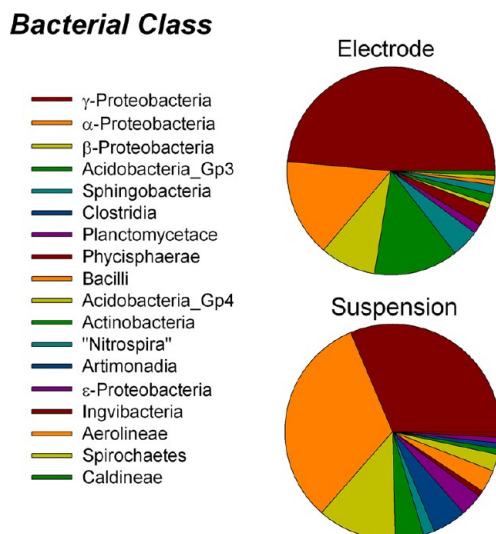


Figure 6. Distribution of bacterial classes between electrode and suspension communities. Taxa were identified from analysis of partial rRNA gene sequences from clone libraries of generated from DNA extracted from samples collected from each community. Results shown are total sequences for three replicate libraries from each community.

reduction,³⁶ which may be important in inorganic N cycling within the algal-bacterial cathode communities. Also within the Xanthomonadaceae, *Pseudofulvimonas* was also present in both communities ($6.7 \pm 3.3\%$ in electrode samples, $2.6 \pm 0.6\%$ in suspended samples). The next most abundant family in the catholyte suspension was the Rhodobacteraceae, representing $24.4 \pm 17.0\%$ of the sequences in the suspended samples but only $1.1 \pm 1.9\%$ in the cathode electrode samples. The most common Rhodobacteraceae genus was *Rhodobacter*, which was abundant ($17.1 \pm 12.5\%$) in the catholyte suspension but rare in the cathode electrode community ($<1\%$ of total sequences). Additional BLAST searches suggested possibly *R. changlensis*, a nonmotile purple nonsulfur bacterium which, like other *Rhodobacter* species, can be photosynthetic.³⁷ Another Rhodobacteraceae genus, *Pannonibacter*, was also well represented ($3.8 \pm 3.3\%$) in suspension but was absent from the cathode electrode. The Acidobacteria_gp3 unclassified family was the second most abundant in the electrode community comprising $13.5 \pm 9.5\%$ of the sequences but only $4.6 \pm 2.3\%$ of the sequences identified in the catholyte suspension samples. Comamonadaceae was the third most abundant bacterial family in the catholyte suspension communities ($12.3 \pm 6.9\%$ of total) and the fourth most common in the communities on the electrode ($5.1 \pm 1.9\%$). This family was dominated by the genus *Hydrogenophaga*, found in both the suspension and the cathode electrode, and known to be a common aquatic and soil bacterium capable of H-oxidation.³⁸ The common soil bacterial genus *Brevundimonas* (Caulobacteraceae) was identified in both the electrode ($4.6 \pm 3.9\%$) and the suspension ($3.5 \pm 1.6\%$) samples. *Brevundimonas* species have been demonstrated to perform enhanced biological phosphorus removal from wastewater³⁹ and provide biomass for removal of heavy metals from wastewater.⁴⁰

An amino-acid utilizing anaerobic bacterium, *Anaeromusa*, and other anaerobes of the class Clostridia (genus *Proteiniclasticum*) were found in suspension samples, but not in the electrode community. This was despite obviously aerobic conditions present due to algal photosynthesis. However, daily

excursions into low oxygen conditions (Figure 1) during the dark phase may have promoted the survival of this bacterium.

Aside from the abundant *Aquimonas*, which could have been involved in the reduction of nitrate to nitrite, other key taxa known to be involved in the nitrogen transformations were identified. *Nitrosomonas* (1.4% of sequences in the electrode samples) can oxidize ammonium to nitrite; *N. europaea* is known to degrade a variety of organic compounds pollutants.⁴¹ *Nitrospira*, also 1.4% of sequences in the electrode samples, could have been oxidizing nitrite to nitrate. Sequences identified as *Mesorhizobium*, a gram-negative soil bacterium, were found in the suspension samples and could indicate the presence of a diazotrophic species; however, high fixed nitrogen concentrations were maintained in the catholyte (e.g., up to $20\text{--}30\text{ mg NO}_3^- \text{-N/L}$), so fixation of N_2 in the cathode would have been unlikely.

Despite the reported abundance of Firmicutes and Bacteroidetes in the sewerage water from South Shore treatment plant,⁴² which was the source of sludge as inoculum for the anode, these phyla were not well represented in the cathode electrode and the suspension communities. Firmicutes were absent from the electrode samples and were only 9.4% of the sequences identified in the suspension communities (comprising Classes Clostridia 5.1% and Bacilli 4.3% of the total suspension sample sequences). This result compares with 76% of the suspension sequences as phylum Proteobacteria. Bacteroidetes were represented as 6.9% of the sequences in the electrode communities but only two sequences in one sample of the suspension community (1.7% of total). Of the Bacteroidetes, Chitinophagaceae and Sphingomonadaceae were the identified families; Sphingomonadaceae was absent from the suspension samples. The low relative abundance of Firmicutes and Bacteroidetes, which are commonly found in MFC anodes,^{43–45} likely resulted from the aerobic condition and the low organic contents in the cathode.

The combined algal and bacterial metabolic activities in the IPB system provide conditions that promote shifts in abundance of the different bacterial taxa. Our future studies will better understand the (cathode) bacterial functions in correlation with the IPB performance (e.g., nutrient removal and algal growth).

■ ASSOCIATED CONTENT

📄 Supporting Information

The methods for calculating Coulombic efficiency, Coulombic recovery, and energy estimation, and the procedures for scanning electron microscopy and cathode microbial analysis are described in the Supporting Information. The standard curve for measurement of the algal power production in the IPB system for more than 360 days and the distribution of the bacterial family and genera are shown in Figure S 1–4. This material is available free of charge via the Internet at <http://pubs.acs.org>.

■ AUTHOR INFORMATION

Corresponding Author

*Phone: (414) 229-5846; fax: (414) 229-6958; e-mail: zhenhe@uwm.edu.

Notes

The authors declare no competing financial interest.

ACKNOWLEDGMENTS

This study was financially supported by a grant from National Science Foundation (award CBET-1033505). We thank Dr. Sandra McLellan (UW-Milwaukee) for her help with microbial sequencing, Dr Heather Owen (UW-Milwaukee) for assistance with Scanning Electron Microscopy, and Dr. Marjorie Piechowski (UW-Milwaukee) for proofreading the manuscript.

REFERENCES

- (1) Logan, B. E. Exoelectrogenic bacteria that power microbial fuel cells. *Nat. Rev. Microbiol.* **2009**, *7*, 375–381.
- (2) Virdis, B.; Rabaey, K.; Rozendal, R. A.; Yuan, Z.; Keller, J. Simultaneous nitrification, denitrification and carbon removal in microbial fuel cells. *Water Res.* **2010**, *44* (9), 2970–2980.
- (3) Logan, B. E.; Hamelers, B.; Rozendal, R.; Schroder, U.; Keller, J.; Freguia, S.; Aelterman, P.; Verstraete, W.; Rabaey, K. Microbial fuel cells: Methodology and technology. *Environ. Sci. Technol.* **2006**, *40* (17), 5181–5192.
- (4) Hoffmann, J. P. Wastewater treatment with suspended and nonsuspended algae. *J. Phycol.* **1998**, *34*, 757–763.
- (5) Pant, D.; Van Bogaert, G.; Diels, L.; Vanbroekhoven, K. A review of the substrates used in microbial fuel cells (MFCs) for sustainable energy production. *Bioresour. Technol.* **2010**, *101* (6), 1533–1543.
- (6) Clauwaert, P.; Rabaey, K.; Aelterman, P.; Schampelaire, L. D.; Pham, T. h.; Boeckx, P.; Boon, N.; Verstraete, W. Biological denitrification in microbial fuel cells. *Environ. Sci. Technol.* **2007**, *41*, 3354–3360.
- (7) Zhang, F.; He, Z. Simultaneous nitrification and denitrification with electricity generation in dual-cathode microbial fuel cells. *J. Chem. Technol. Biotechnol.* **2012**, *87* (1), 153–159.
- (8) Cusick, R. D.; Logan, B. E. Phosphate recovery as struvite within a single chamber microbial electrolysis cell. *Bioresour. Technol.* **2012**, *107*, 110–115.
- (9) Kuntke, P.; Śmiech, K. M.; Bruning, H.; Zeeman, G.; Saakes, M.; Sleutels, T. H. J. A.; Hamelers, H. V. M.; Buisman, C. J. N. Ammonium recovery and energy production from urine by a microbial fuel cell. *Water Res.* **2012**, *46* (8), 2627–2636.
- (10) Ugwu, C. U.; Aoyagi, H.; Uchiyama, H. Photobioreactors for mass cultivation of algae. *Bioresour. Technol.* **2008**, *99* (10), 4021–4028.
- (11) Muñoz, R.; Guieysse, B. Algal–bacterial processes for the treatment of hazardous contaminants: A review. *Water Res.* **2006**, *40* (15), 2799–2815.
- (12) Chisti, Y. Biodiesel from microalgae. *Biotechnol. Advances* **2007**, *25* (3), 294–306.
- (13) Rittmann, B. E. Opportunities for renewable bioenergy using microorganisms. *Biotechnol. Bioeng.* **2008**, *100* (2), 203–212.
- (14) Strik, D. P. B. T. B.; Terlouw, H.; Hamelers, H. V. M.; Buisman, C. J. N. Renewable sustainable biocatalyzed electricity production in a photosynthetic algal microbial fuel cell (PAMFC). *Appl. Microbiol. Biotechnol.* **2008**, *81* (4), 659–668.
- (15) Velasquez-Orta, S. B.; Curtis, T. P.; Logan, B. E. Energy from algae using microbial fuel cells. *Biotechnol. Bioeng.* **2009**, *103* (6), 1068–1076.
- (16) Zhang, Y.; Noori, J. S.; Angelidaki, I. Simultaneous organic carbon, nutrients removal and energy production in a photomicrobial fuel cell (PFC). *Energy Environ. Sci.* **2011**, *4*, 4340–4346.
- (17) He, Z.; Kan, J.; Mansfeld, F.; Angenent, L. T.; Neelson, K. H. Self-sustained phototrophic microbial fuel cells based on the synergistic cooperation between photosynthetic microorganisms and heterotrophic bacteria. *Environ. Sci. Technol.* **2009**, *43* (5), 1648–1654.
- (18) Xiao, L.; Damien, J.; Luo, J.; Jang, H. D.; Huang, J.; He, Z. Crumpled graphene particles for microbial fuel cell electrodes. *J. Power Sour.* **2012**, *208*, 187–192.
- (19) Park, J. B. K.; Craggs, R. J. Wastewater treatment and algal production in high rate algal ponds with carbon dioxide addition. *Water Sci. Technol.* **2010**, *61* (3), 633–639.
- (20) Rozendal, R. A.; Hamelers, H. V. M.; Buisman, C. J. N. Effects of membrane cation transport on pH and microbial fuel cell performance. *Environ. Sci. Technol.* **2006**, *40*, 5206–5211.
- (21) Park, J. B. K.; Craggs, R. J.; Shilton, A. N. Wastewater treatment high rate algal ponds for biofuel production. *Bioresour. Technol.* **2011**, *102* (1), 35–42.
- (22) Fornero, J. J.; Rosenbaum, M.; Cotta, M. A.; Angenent, L. T. Carbon dioxide addition to microbial fuel cell cathodes maintains sustainable catholyte pH and improves anolyte pH, alkalinity, and conductivity. *Environ. Sci. Technol.* **2010**, *44*, 2728–2734.
- (23) Fan, Y.; Hu, H.; Liu, H. Sustainable power generation in microbial fuel cells using bicarbonate buffer and proton transfer mechanisms. *Environ. Sci. Technol.* **2007**, *41*, 8154–8158.
- (24) He, Z.; Kan, J.; Wang, Y.; Huang, Y.; Mansfeld, F.; Neelson, K. H. Electricity production coupled to ammonium in a microbial fuel cell. *Environ. Sci. Technol.* **2009**, *43* (9), 3391–3397.
- (25) Chan, K.-y.; Wong, K. H.; Wong, P. K. Nitrogen and phosphorus removal from sewage effluent with high salinity by *Chlorella Salina*. *Environ. Pollut.* **1979**, *18*, 139–146.
- (26) Dortch, Q. The interaction between ammonium and nitrate uptake in phytoplankton. *Mar. Ecol. Prog. Ser.* **1990**, *61*, 183–201.
- (27) Chisholm, S. W. Temporal patterns of cell division in unicellular algae. *Can. Bull. Fish Aquat. Sci.* **1981**, *210*, 150–181.
- (28) Choi, O.; Das, A.; Yu, C.-P.; Hu, Z. Nitrifying bacterial growth inhibition in the presence of algae and cyanobacteria. *Biotechnol. Bioeng.* **2010**, *107* (6), 1004–1011.
- (29) Molina, E.; Fernandez, J.; Acien, F. G.; Chisti, Y. Tubular photobioreactor design for algal cultures. *J. Biotechnol.* **2001**, *92*, 113–131.
- (30) Chisti, Y. Biodiesel from microalgae beats bioethanol. *Trends Biotechnol.* **2008**, *26* (3), 126–131.
- (31) Kim, J.; Kim, K.; Ye, H.; Lee, E.; Shin, C.; McCarty, P. L.; Bae, J. Anaerobic fluidized bed membrane bioreactor for wastewater treatment. *Environ. Sci. Technol.* **2011**, *45*, 576–581.
- (32) Force, J. T., *Design of Municipal Wastewater Treatment Plants: WEF Manual of Practice No.8*; Water Environment Federation: Alexandria, 1998.
- (33) Kim, J.; Kim, K.; Ye, H.; Lee, E.; Shin, C.; McCarty, P. L.; Bae, J. Anaerobic fluidized bed membrane bioreactor for wastewater treatment. *Environ. Sci. Technol.* **2011**, *45* (2), 576–81.
- (34) McCarty, P. L.; Bae, J.; Kim, J. Domestic wastewater treatment as a net energy producer—Can this be achieved? *Environ. Sci. Technol.* **2011**, *45* (17), 7100–7106.
- (35) Logan, B.; Regan, J. Electricity-producing bacterial communities in microbial fuel cells. *Trends Microbiol.* **2006**, *14* (12), 512–518.
- (36) LaSala, P. R.; Segal, J.; Han, F. S.; Tarrand, J. J.; Han, X. Y. First reported infections caused by three newly described genera in the family Xanthomonadaceae. *J. Clin. Microbiol.* **2007**, *45* (2), 641–644.
- (37) Anil Kumar, P.; Srinivas, T. N.; Sasikala, C.; Ramana, Ch, V. *Rhodobacter changlensis* sp. nov., a psychrotolerant, phototrophic alphaproteobacterium from the Himalayas of India. *Int. J. Syst. Evol. Microbiol.* **2007**, *57* (Pt 11), 2568–71.
- (38) Yoon, K. S.; Tsukada, N.; Sakai, Y.; Ishii, M.; Igarashi, Y.; Nishihara, H. Isolation and characterization of a new facultatively autotrophic hydrogen-oxidizing Betaproteobacterium, *Hydrogenophaga* sp. AH-24. *FEMS Microbiol Lett* **2008**, *278* (1), 94–100.
- (39) Ryu, S. H.; Park, M.; Lee, J. R.; Yun, P. Y.; Jeon, C. O. *Brevundimonas aveniformis* sp. nov., a stalked species isolated from activated sludge. *Int. J. Syst. Evol. Microbiol.* **2007**, *57* (Pt 7), 1561–1565.
- (40) Singh, N.; Gadi, R. Bioremediation of Ni(II) and Cu(II) from wastewater by the nonliving biomass of *Brevundimonas vesicularis*. *J. Environ. Chem. Ecotoxicol.* **2012**, *4* (8), 137–142.
- (41) Chain, P.; Lamerdin, J.; Larimer, F.; Regala, W.; Lao, V.; Land, M.; Hauser, L.; Hooper, A.; Klotz, M.; Norton, J.; Sayavedra-Soto, L.; Arciero, D.; Hommes, N.; Whittaker, M.; Arp, D. Complete genome sequence of the ammonia-oxidizing bacterium and obligate chemolithoautotroph *Nitrosomonas europaea*. *J. Bacteriol.* **2003**, *185* (9), 2759–2773.

(42) McLellan, S. L.; Huse, S. M.; Mueller-Spitz, S. R.; Andreishcheva, E. N.; Sogin, M. L. Diversity and population structure of sewage-derived microorganisms in wastewater treatment plant influent. *Environ. Microbiol.* **2010**, *12* (2), 378–392.

(43) Sun, Y.; Wei, J.; Liang, P.; Huang, X. Electricity generation and microbial community changes in microbial fuel cells packed with different anodic materials. *Bioresour. Technol.* **2011**, *102* (23), 10886–10891.

(44) Kan, J.; Hsu, L.; Cheung, A. C.; Pirbazari, M.; Neelson, K. H. Current production by bacterial communities in microbial fuel cells enriched from wastewater sludge with different electron donors. *Environ. Sci. Technol.* **2011**, *45* (3), 1139–1146.

(45) Ishii, S.; Suzuki, S.; Norden-Krichmar, T. M.; Neelson, K. H.; Sekiguchi, Y.; Gorby, Y. A.; Bretschger, O. Functionally stable and phylogenetically diverse microbial enrichments from microbial fuel cells during wastewater treatment. *PLoS One* **2012**, *7* (2), e30495.